PAPER

Induced spin–orbit splitting in graphene: the role of atomic number of the intercalated metal and π–d hybridization

New Journal of Physics
The open access journal for physics

Induced spin–orbit splitting in graphene: the role of atomic number of the intercalated metal and π–d hybridization

Alexander M Shikin[1,3], Artem G Rybkin[1], Dmitry Marchenko[1,2], Anna A Rybkina[1], Markus R Scholz[2], Oliver Rader[2] and Andrei Varykhalov[2]

[1] Physics Faculty, St Petersburg State University, ul. Ulyanovskaya 1, 198504 St Petersburg, Peterhof, Russia
[2] Helmholtz-Zentrum Berlin für Materialien und Energie, Elektronenspeicherring BESSY II, Albert-Einstein-Straße 15, D-12489 Berlin, Germany
E-mail: shikin@paloma.spbu.ru

New Journal of Physics **15** (2013) 013016 (18pp)
Received 10 March 2012
Published 9 January 2013
Online at http://www.njp.org/
doi:10.1088/1367-2630/15/1/013016

Abstract. This paper reports spin-dependent valence-band dispersions of graphene synthesized on Ni(111) and subsequently intercalated with monolayers of Au, Cu and Bi. We have previously shown that after intercalation of graphene with Au the dispersion of the π band remains linear in the region of the $\bar{K}$ point of the surface Brillouin zone even though the system exhibits a noticeable hybridization between π states of graphene and d states of Au. We have also demonstrated a giant spin–orbit splitting of π states in Au-intercalated graphene which can reach up to ∼100 meV. In this paper we probe in detail dispersions of graphene π–Au d hybridized bands. We show that intercalation of Cu does not produce a noticeable spin–orbit splitting in graphene although this system, similarly to Au-intercalated graphene, also reveals hybridization between graphene states and d states of Cu. To clarify the role of intercalated Au, the electronic and spin structures of Au monolayers on Ni(111) are comparatively studied with and without graphene on top and the importance of the spin splitting of the d states of the intercalated material is established.

[3] Author to whom any correspondence should be addressed.

These Au d states in graphene/Au/Ni(111) are further studied in detail by spin- and angle-resolved photoemission, and spin-dependent hybridization between graphene and Au bands is revealed. In contrast, intercalation of the sp metal Bi, despite its high atomic number, does not lead to any measurable spin–orbit splitting of the π states of graphene. This means that for the creation of large spin–orbit splitting in graphene, neither hybridization with d states (as with Cu) nor the high atomic number of the intercalated material alone (as with Bi) is sufficient, and a combination of them is required (as with Au).

Contents

1. Introduction **2**
2. Experimental techniques **3**
3. Results of the experiments **4**
4. Discussion **10**
5. Conclusion **16**
Acknowledgments **17**
References **17**

1. Introduction

The deep present-day interest of researchers in the electronic properties of graphene layers and graphene-based compounds was primarily prompted by the specific features of the two-dimensional structure of graphene and by the fascinating effects not observable in conventional three-dimensional materials [1–9]. It has been established that electronic states in free-standing graphene exhibit a characteristic photon-like linear dispersion near the $\bar{K}$ point of the surface Brillouin zone (SBZ) in the vicinity of the Fermi energy [7–11]. It is the linearity of the dispersion relations which accounts for a variety of unique phenomena inherent in graphene, such as the Klein paradox [5, 7] and the half-integer quantum Hall effect [3, 4], which were observed to vanish in few-layer graphene samples. That is why the formation of graphene coatings retaining the unique characteristics of free-standing graphene along with the development of well-reproducible methods for growth of single-layer graphene are problems under the focus of current research.

We recently demonstrated the possibility of using contact with a monolayer of Au to create a large spin–orbit splitting in the graphene π states [10], which renders graphene a promising material for applications in spintronic devices. The Au-induced splitting reaches a giant value of $\sim$100 meV [11], which is remarkable, since the intrinsic spin–orbit splitting in free-standing graphene is very small ($<$0.1 meV [12]). Interestingly, recent studies [13–17] have demonstrated, for metal-on-metal films, that giant spin–orbit splitting of electronic states localized in thin adsorbed layers may be created due to the high atomic number of the substrate material. In particular, it has been shown that upon deposition of thin films of Au, Ag, Cu [13–15] and Al [16, 17] on the W(110) surface, a giant spin–orbit splitting is induced by the substrate in interface and quantum-well states of the adlayers. It has been demonstrated that the magnitude of such an induced spin–orbit splitting is practically independent of the atomic number of the adsorbed material and is explicitly determined by the electronic structure of the

substrate and its atomic number. It is remarkable that even in the case of a very light Al layer, the magnitude of the induced spin–orbit splitting of electronic states was extremely large [16, 17]. Deposition of the same materials on the Mo(110) surface, the atomic and electronic structure of which is almost identical to W(110) but with smaller atomic number, results in a substantial decrease of the magnitude of the substrate-induced spin–orbit splitting in the adlayers [13]. In other words, deposition of metals on a substrate with a smaller atomic number brings about a smaller induced spin–orbit splitting.

The present study compares the substrate-induced spin–orbit splitting in graphene (i.e. an element with a low atomic number ($Z_C = 6$)) intercalated with a monolayer of Au (i.e. a high-atomic-number element, $Z_{Au} = 79$)) with spin–orbit splitting in graphene intercalated with a monolayer of Cu (i.e. a metal with a substantially lower atomic number, $Z_{Cu} = 29$). Band structures acquired by means of angle-resolved photoemission reveal that graphene π states strongly hybridize with the d states of Au [11] and Cu. Spin-resolved photoemission measurements show that this hybridization is spin dependent and responsible for the spin–orbit splitting in graphene [11]. We follow here its behavior in detail. We have been able to show that intercalation of a Au monolayer under graphene does initiate an anomalously large spin–orbit splitting of the graphene π states, which differs between energy–momentum regions where graphene π states cross the Au d states and the region near the $\bar{K}$ point of the SBZ where the graphene dispersion is linear (outside the crossing region). A significant role was found to be played by hybridization of the π states of graphene with the Au 5d states and by the corresponding spin-dependent avoided crossing of electronic bands [11]. For the purpose of comparison, we measured the magnitude of the spin–orbit splitting in graphene intercalated with a monolayer of Cu and found that it is substantially smaller, almost unobservable in the experiment. The role of the intrinsic spin–orbit splitting of Au 5d states in intercalated monolayers was analyzed by a comparative characterization of Au/Ni(111) without graphene on top. In addition, we show that intercalation of the heavy metal Bi ($Z_{Bi} = 84$) without d electrons in the valence band does not create any substantial induced spin–orbit splitting of π states in graphene. This fact emphasizes not only the importance of a high atomic number of the intercalated material but also the necessity of hybridization between π states of graphene and d states of the underlying metal.

2. Experimental techniques

The experiments were performed at the Russian–German PGM, U125/2-SGM and UE112-PGM1 beamlines at BESSY-II (Helmholtz-Zentrum Berlin). Graphene was prepared by catalytic cracking of propylene on annealed Ni(111) layers at a temperature of 750 K. The intercalation of Au, Cu and Bi monolayers was done by deposition of the materials on graphene synthesized on Ni(111), followed by annealing the sample at 700 K. The propylene-cracking-based synthesis of graphene on a Ni substrate, with subsequent intercalation of atoms of noble metals, was developed and first described in [18] and was subsequently refined [19–29]. Intercalation of Bi is reported for the first time in the present work. Unlike the original experiments, in the actual study graphene was synthesized on a ∼100 Å-thick Ni(111) film grown epitaxially on the W(110) single-crystal surface. Such a preparation method complemented by an analysis of the specific features inherent in the electronic and atomic structure of the sample is reported in detail in [10]. In this work, the electronic and spin structure of the investigated systems is studied with the help of angle- and spin-resolved photoemission

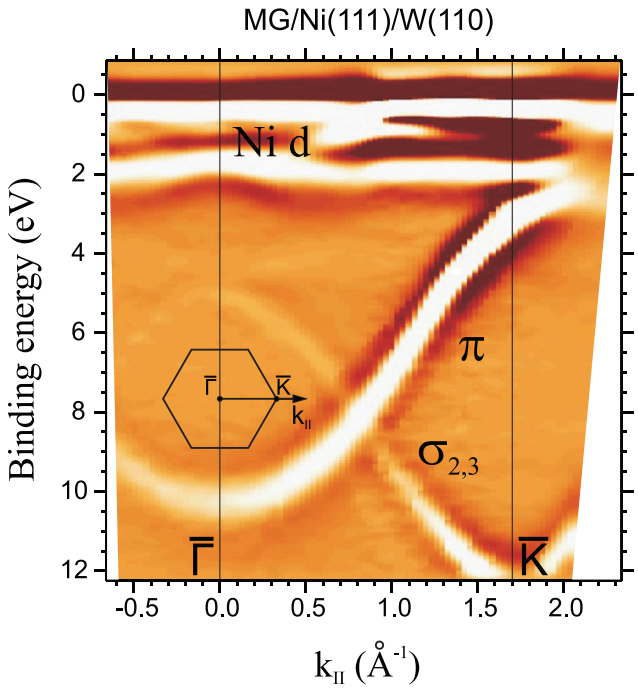

Figure 1. Dispersion of graphene and Ni valence-band electronic states along the $\bar{\Gamma}\bar{K}$ direction of the SBZ for graphene synthesized on a thin Ni(111) film. The inset shows the SBZ structure. The arrow specifies the direction along which the dispersion was measured. In order to emphasize the dispersion, the second derivate of photoemission intensity by energy is shown.

spectroscopy. The spin-resolved measurements were carried out with a Phoibos hemispherical energy analyzer equipped with a Mott spin polarimeter operated at 26 keV. The angle- and spin-resolved dispersions of the valence-band electronic states were measured with linearly polarized light at a photon energy of 62 eV. The studies were carried out in ultrahigh vacuum (base pressure 1×10^{-10} mbar) at room temperature. High-resolution measurements of the graphene π state dispersions near the $\bar{K}$ point of the SBZ were carried out at a temperature of 40 K, with all three angles of sample orientation precisely tuned.

3. Results of the experiments

Figures 1 and 2 compare the dispersion of the π states in graphene synthesized by cracking of propylene on Ni(111) with the dispersion obtained after intercalation of an Au monolayer between graphene and Ni. The spectra were measured along the $\bar{\Gamma}\bar{K}$ direction of the SBZ in the polar angles covering the region 0–27°, which corresponds to the first SBZ of graphene ($k_{\parallel} = 0$–1.7 Å^{-1}).

The electronic structure of graphene synthesized on Ni(111) features a noticeable shift of the valence band structure as a whole toward higher binding energy as compared to free-standing graphene or crystalline graphite [10, 22, 23]. Figure 3 displays normal emission photoelectron spectra for bare graphene/Ni(111) and after its intercalation with a monolayer of Au, Cu and Bi. As seen from normal emission spectra as well as from the dispersion relations in bare graphene on Ni(111) the binding energy of the π states near the $\bar{\Gamma}$ point is ~10 eV, while at the $\bar{K}$ point

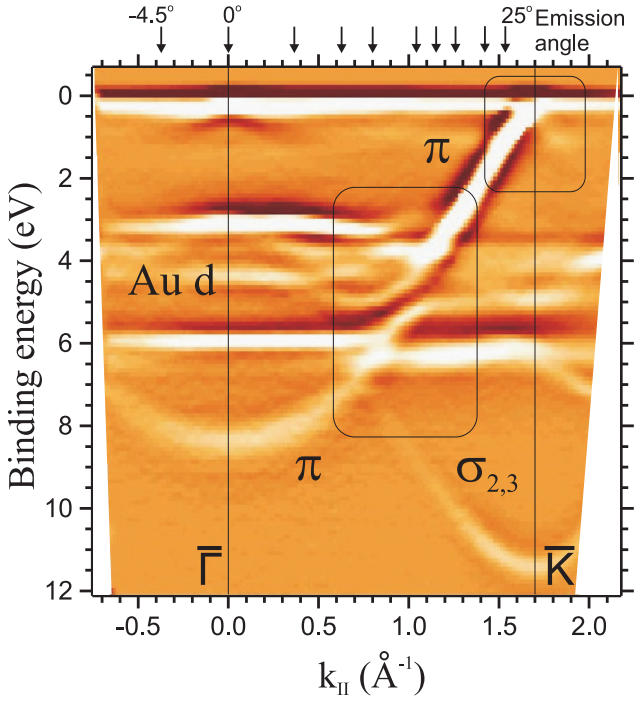

Figure 2. Band structure of graphene on Ni(111) intercalated with a monolayer of Au. The dispersion is measured along the $\bar{\Gamma}\bar{K}$ direction of the SBZ. Regions denoted with frames are zoomed in figure 4. In order to emphasize the dispersion, the second derivate of photoemission intensity by energy is shown. Arrows indicate the polar angles for which spin-resolved spectra have been measured (see figures 5).

of the SBZ the π states come only as close as $\sim$2 eV to the Fermi level and hybridize there with Ni d states. This shows convincingly that synthesized graphene is strongly coupled to the Ni substrate. This coupling has a covalent nature [18–21, 25] and is accompanied by different shifts of the π and σ states, which can be ascribed to the corresponding wave functions being hybridized to different extents. In the energy region of Ni d states, a large gap opens up in the dispersion of graphene bands due to electronic hybridization between graphene and Ni. The branch of empty π^* states is lying above the Fermi level and is not probed by photoemission.

Intercalation of Au atoms (figure 2) decouples graphene from the substrate, shifting the band structure noticeably toward lower binding energies [10, 22], as is the case with other noble metals as well [23–25, 27]. Such an effect occurs also upon intercalation of Au underneath graphene on SiC(0001) [30] and Ru(0001) [31]. Noticeable weakening of the coupling between graphene and Ni(111) upon intercalation of noble metals was also observed in phonon spectra [18–21]. Figure 4(a) shows on an enlarged scale the measured dispersion of the π band in graphene intercalated with Au near the $\bar{K}$ point of the SBZ. One can clearly see that after intercalation of Au the dispersion relation becomes linear [27]. Unlike the dispersion relations plotted in figure 2, the curves in figure 4(a) were measured along the direction passing through the $\bar{K}$ point, but perpendicular to the $\bar{\Gamma}$–$\bar{K}$ direction of the SBZ (see the sketch in the inset of figure 4(a)) [10, 27]. At this detection geometry, final-state diffraction of photoelectrons is suppressed and both branches of the π band dispersion are seen equally well. Importantly, the Dirac energy where cones of filled and empty states touch each other is practically

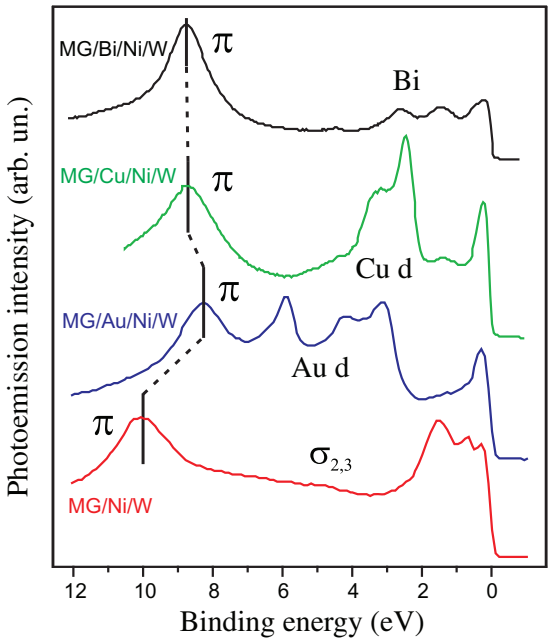

Figure 3. Photoemission spectra measured in normal emission with an angular resolution of ∼0.5° for bare monolayer graphene (MG) on Ni(111) (MG/Ni/W) and for graphene intercalated with monolayers of Au, Cu and Bi (MG/Au/Ni/W, MG/Cu/Ni/W, MG/Bi/Ni/W).

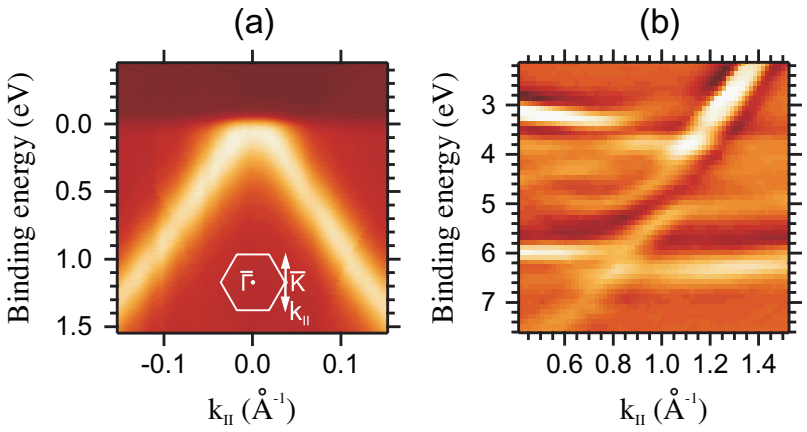

Figure 4. Zoomed dispersions of the π states in graphene intercalated with Au monolayer and measured (a) in the vicinity of the $\bar{K}$ point of the SBZ and (b) in the region where graphene π states are crossing with Au 5d states. Arrows in (a) specify the direction within the SBZ along which the dispersion of the π band with $k_{\|}$ was measured. These regions are those denoted by frames in figure 2. The Dirac cone shown in (a) was recorded at 40 K.

equal to the Fermi energy. We clearly see that graphene arranged on top of an intercalated layer of Au retains the unique features of the electronic structure characteristic of isolated free-standing graphene.

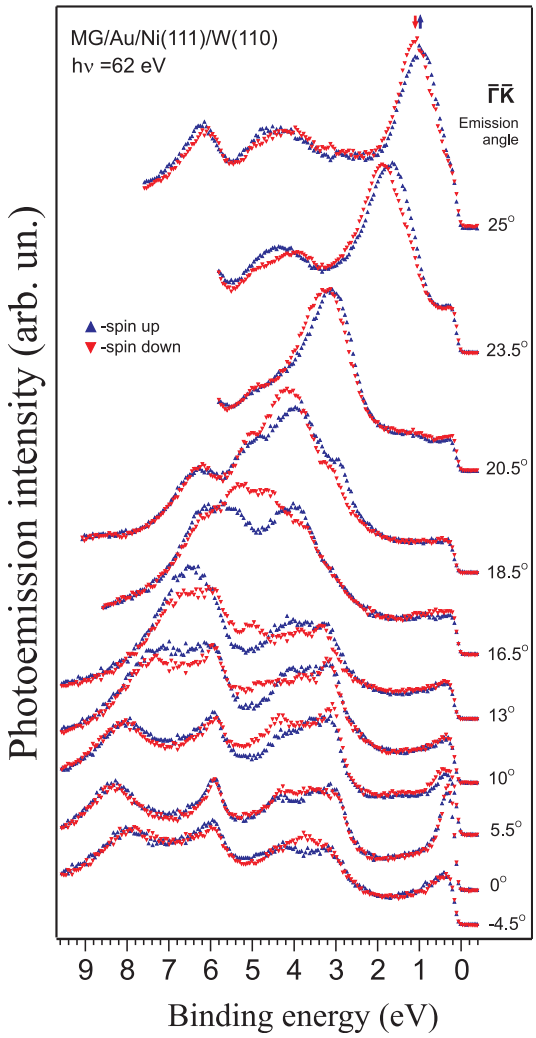

Figure 5. Series of spin-resolved photoemission spectra for Au-intercalated graphene monolayer measured along the $\bar{\Gamma}\bar{K}$ direction in the SBZ for different emission angles (wavevectors $k_{\|}$). The contributions of states with oppositely oriented spins are denoted with blue and red colors.

Besides the graphene π states, the dispersion relations measured over the whole SBZ and displayed in figure 2 reveal the presence of Au 5d states in the 2.5–7 eV energy region. Figure 4(b) shows in greater detail the energy-momentum region where the Au 5d bands cross the π states of graphene. Analysis of the dispersion relations clearly demonstrates a substantial distortion of the graphene π band upon crossing with Au bands, resulting in the formation of local energy gaps. The observed pronounced modification of the band structure can be assigned to the hybridization between π states of graphene and 5d states of Au, which results in the formation of corresponding (d–π) bonding and (d–π)* antibonding hybridized states at the energies below and above the region where dispersions of Au and graphene cross.

These hybridization phenomena have been shown to affect the spin structure of graphene [11]. Figures 5, 6(a) and (b) display detailed spin-resolved photoemission spectra measured for different polar angles (different wavevectors $k_{\|}$ from Au-intercalated graphene on

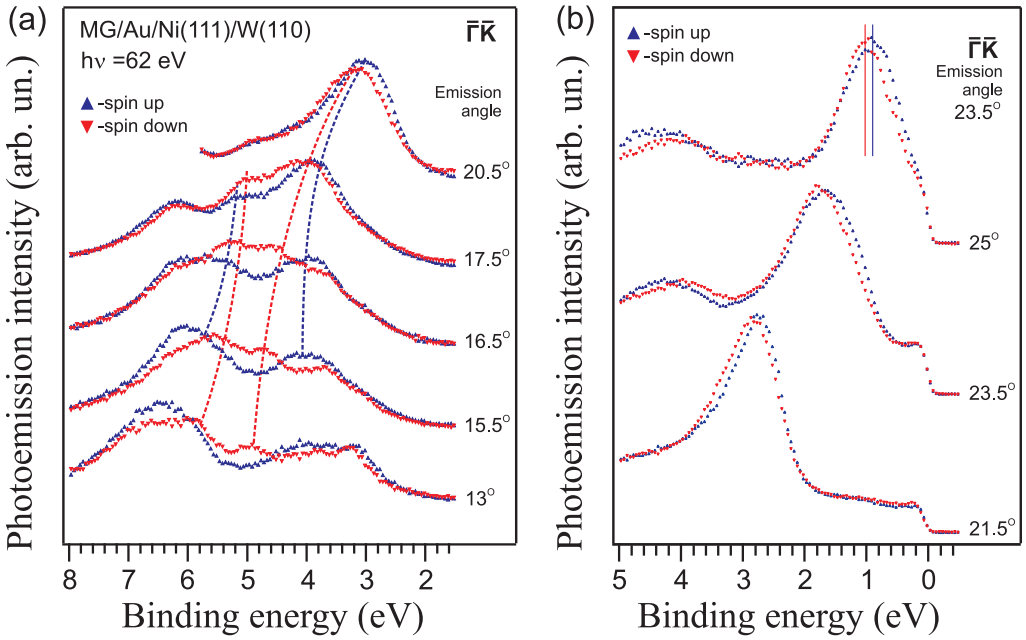

Figure 6. Spin-resolved photoemission spectra for Au-intercalated graphene measured (a) for polar angles corresponding to the region of hybridization between graphene π states and 5d states of Au, which demonstrate the spin-dependent avoided band crossing and the pronounced modification of the spin structure of graphene π states and (b) for polar angles corresponding to the electronic wavevectors close to the $\bar{K}$ point of the SBZ, i.e. in the region where the dispersion of the graphene π states is linear. The contributions due to states with opposite spins are specified by blue and red triangles and corresponding dashed lines.

Ni(111)). The spectra with oppositely oriented spins are shown in blue and red. As seen from these spectra, in the region where the graphene states cross the Au 5d states the spin structure of the system undergoes a substantial modification. The π states with oppositely oriented spins split at the band crossing point to follow the dispersion of 5d states of Au. The spin splitting of the Au 5d states themselves is clearly seen at polar angles of 23–25° and 5–10° relative to the surface normal (this corresponds to the $k_{\|} = 1.5$–1.7 and 0.3–$0.6\,\text{Å}^{-1}$, respectively) where Au states are energetically separated from the graphene band. The observed changes in the spin structure allow for a description in terms of the spin-dependent avoided crossing between graphene π and Au 5d states. The spin splitting of the graphene π states is observed up to the Fermi energy [11]. Figure 6(b) zooms spin-resolved spectra of π states and emphasizes how the spin splitting of the graphene band persists in the region near the $\bar{K}$ point of the SBZ and up to the Fermi energy. The observed spin splitting in this region reaches a value of about 100 meV [11]. At the same time the linearity of the graphene dispersion is not affected.

To elucidate the role played by the substrate and by its atomic number for the observed effects of induced spin–orbit interaction in graphene, the spin splitting was studied in graphene intercalated with a monolayer of another noble metal, namely Cu, which has an electronic configuration similar to Au but a much smaller atomic number.

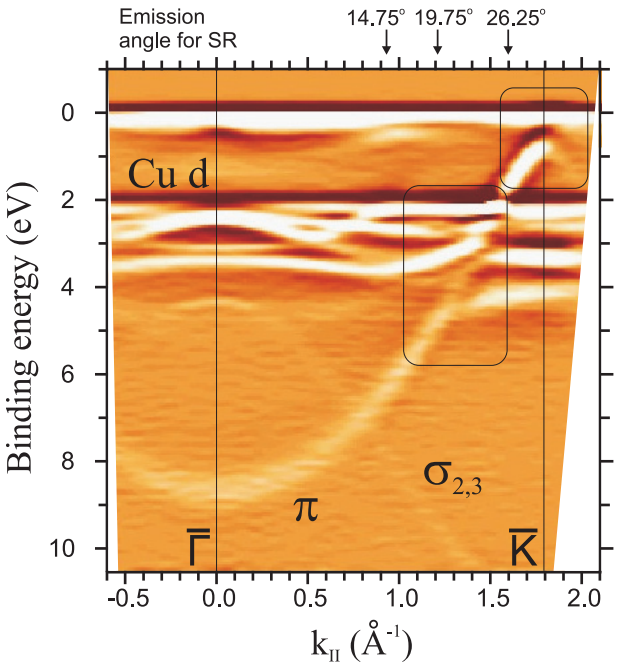

Figure 7. Dispersion of valence band electronic states of graphene and Cu along the $\bar{\Gamma}\bar{K}$ direction of the Brillouin zone measured for a graphene monolayer intercalated by a Cu monolayer. Rectangles mark the regions displayed in close-up in figure 8. To make the dispersion relations more revealing, they are visualized in the form of the second derivative of the photoemission spectra. Arrows indicate the polar angles for which spin-resolved spectra have been measured (see figure 9).

Figure 7 demonstrates the dispersion of the valence-band electronic states in Cu-intercalated graphene synthesized on the Ni(111) surface. Figure 8(a) reports on a finer scale the dispersion of π states in the vicinity of the Fermi level close to the $\bar{K}$ point of the SBZ. It is evident from the dispersions shown that in Cu-intercalated graphene the π band overall follows the pattern observed for graphene intercalated with Au. One also sees a noticeable shift of the π band by 1–1.5 eV toward the Fermi level as compared to the bare graphene on Ni(111). In the normal emission spectrum the π states appear at $\sim$8.75 eV binding energy, which is substantially lower than in the case of bare graphene on Ni. In contrast to Au-intercalated graphene, the Dirac point in Cu-intercalated graphene is found somewhat below the Fermi level. The lower Dirac cone of the filled π states ends at $\sim$0.4 eV binding energy [25, 27] and partial filling of the upper cone of π^* states is observed. A small energy gap of $\sim$180 meV opens up between the upper and lower cones [25, 27]. The Dirac point, identified as the midpoint of the energy gap, is found at $\sim$0.3 eV binding energy. Figure 8(b) shows in greater detail the energy–momentum frame where crossing of the graphene π states with the Cu 3d states takes place [27]. An analysis of the dispersions presented in figures 7 and 8(b) suggests that also in the case of intercalated Cu the π states of graphene hybridize with the 3d states of the noble metal which are located at binding energies of 2–4.5 eV. In the crossing region between the π band of graphene and the 3d of Cu, one again observes a substantial distortion of the band dispersions and appearance of local energy gaps. We face now the same question as in the case with intercalated Au, namely, how the electronic hybridization between graphene

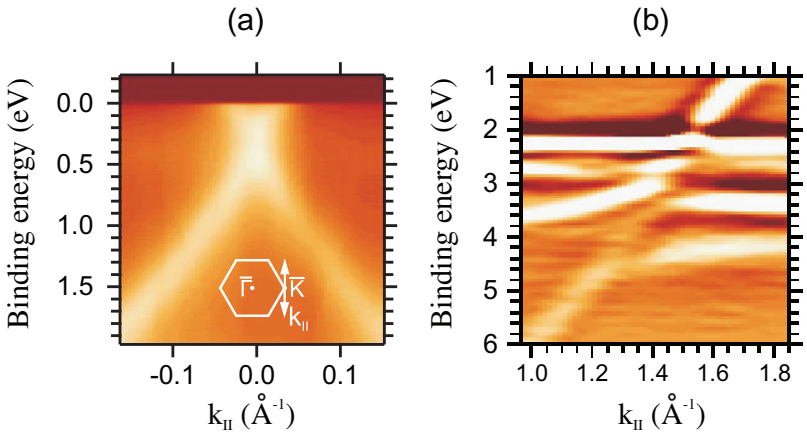

Figure 8. Close-ups of dispersion relations of the π states of graphene intercalated with a Cu monolayer and measured (a) near the $\bar{K}$ point of the Brillouin zone and (b) in the region of the graphene π states crossing with the 3d states of Cu. Arrows in (a) identify the directions of the changes in $k_{\|}$ for which the π state dispersions were measured. These regions correlate with the ones bounded with squares in figure 2. The graph displayed in (a) was recorded at 40 K.

and Cu affects the spin structure of the system. Figure 9 plots the corresponding spin-resolved photoemission spectra measured at different polar angles (different wavevectors $k_{\|}$) from the Cu-intercalated graphene monolayer. We clearly see that despite the pronounced hybridization between graphene and the Cu 3d states, there is no measurable spin splitting in the π band of graphene, neither in the energy–momentum frame where the graphene state crosses the 3d band of Cu nor in the region close to the Fermi energy where the dispersion of the π states is linear. This shows that contact to metals with a low atomic number does not create any noticeable spin–orbit splitting in graphene. This also makes us recall the case of graphene on bare Ni(111) where induced spin–orbit effects are not observed [26, 28] owing to the low atomic number of Ni ($Z_{\mathrm{Ni}} = 28$).

4. Discussion

We start our discussion with an analysis of the specific features of the electronic structure of the investigated systems. What kind of interaction may be responsible for the coupling of graphene to the intercalated monolayers of Au and Cu? And does the pronounced hybridization between the π states of graphene and d states of Au and Cu, accompanied by noticeable distortions of the graphene band structure, not break the linear dispersion of the graphene π states at the $\bar{K}$ point of the SBZ?

It is well known that covalent interaction causes hybridization of electronic states and formation of corresponding hybridized bonding and antibonding states at binding energies below and above the energy where the bands of the states involved in hybridization are crossing. This also results in the formation of local energy gaps, as was observed for graphene π states interacting with d states of Au and Cu (see figures 2, 4(a), 7 and 8(b), respectively). Figure 10 schematically represents such changes in the electronic structure along with the formation of the corresponding bonding and antibonding (d–π) states. The actual strength of

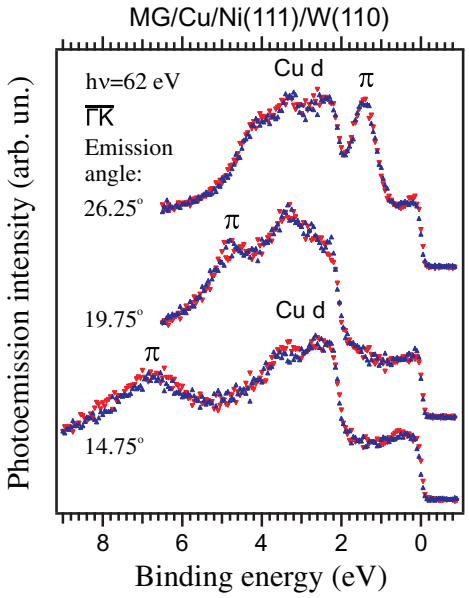

Figure 9. Spin-resolved photoemission spectra obtained for a Cu-intercalated graphene monolayer at different polar angles to the surface normal. The contributions due to different spin directions are identified with blue and red colors.

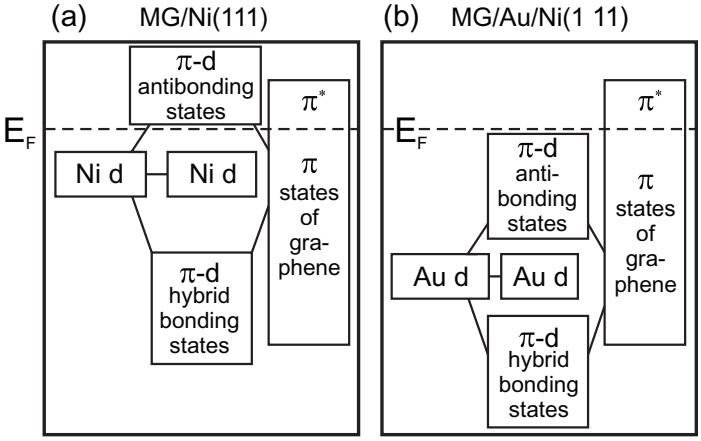

Figure 10. Schematic diagram of the formation and localization in energy of the bonding and antibonding (π–d) states initiated by graphene interaction with (a) Ni and (b) Au.

the covalent coupling emerging between the graphene and the Au (or Cu) layer is mediated by the relative population of the bonding and antibonding states. In the case of graphene on Ni(111) (figure 10(a)) only the bonding states are populated, the covalent bonding is very strong and a wide gap is formed between the bonding and antibonding states (see the region of the $\bar{K}$ point in figure 1).

The studies presented in [32, 33] show convincingly that the states observed at the binding energies of 0–2 eV (i.e. between the π band and the Fermi level) essentially derive from the hybridized (d–π) states. Calculations suggest that the hybridization between π states of graphene and 3d states of Ni initiates a shift of the π band toward higher binding energies.

Importantly, the experimentally observed energetic position of the bottom and top of the π band is reached when the carbon atoms occupy the top-fcc (face centered cubic) configuration with respect to the relatively lower-lying atoms of Ni (i.e. at maximum overlap of the corresponding wavefunctions and strongest hybridization with the Ni 3d states). This description is no different from the picture of covalent interaction between graphene and Ni substrate noted above. Bertoni *et al* [32] and Dedkov and Fonin [33] state that the covalent coupling is accompanied by a charge transfer from Ni to the hybridized interface states located in the vicinity of the Fermi level, which were assumed to create spin polarization in the π states of graphene and induce a magnetic moment in the carbon due to the exchange interaction in Ni. However, the results presented in the present paper, as well as in our earlier publications [10, 22, 25–28], do not support a charge transfer from Ni to graphene which would create spin polarization of the graphene bands. The increase of binding energy of the C 1s core level to 284.9 eV (as compared to 284.5 eV, a value characteristic of highly oriented pyrolitic graphite (HOPG)) does not provide a solid ground for this conclusion about charge transfer, particularly in view of the change in relaxation energies between these two systems. We have neither observed any filling of the π^* states of graphene in the course of its synthesis on Ni nor verified experimentally the exchange-type spin polarization of the π states in graphene grown on the surfaces of magnetized Ni(111) and Co(0001) films [28].

Unlike the situation with Ni-mediated hybridization discussed above, in the cases when the d states of the substrate couple with graphene at higher binding energy (see the schematic diagram in figure 10(b)), the resulting bonding and antibonding states have comparable populations. As a result, the contributions of the bonding and antibonding states to the coupling are largely compensated, which results in significant weakening of the bonding force. It is exactly this effect that occurs in the interaction between graphene and d states of Au and Cu. As compared to Ni, the Au and Cu d states have a higher binding energy and completely filled electronic shells. The antibonding $(\mathrm{d}\text{–}\pi)^*$ states evolving at the binding energies above the region of band crossings also turn out to be almost filled. Exactly this accounts for weak overall coupling between graphene and intercalated Au and Cu layers and the persistence of linearity in the dispersion of the graphene band near the $\bar{\mathrm{K}}$ point of the SBZ.

After the intercalation of Au, the overall weakness of the graphene coupling to the substrate makes the electronic structure of graphene states close to the Fermi energy similar to that of free-standing graphene [10] with Dirac cones of π and π^* states touching in the vicinity of the Fermi level. Moreover, in the Cu-intercalated graphene, an energy shift of the π band as a whole toward higher binding energies and formation of a small energy gap near the Fermi level are observed [27]. A similar shift and opening of a band gap takes place for graphene grown by evaporation of carbon atoms on a Cu(111) single crystal [34]. By comparison with those results, we can conclude that the underlying Ni layer does not significantly influence the electronic structure of the graphene after intercalation.

As was noted before, the shift of the whole band structure of Cu-intercalated graphene toward higher binding energies (as compared to Au-intercalated graphene) can be ascribed to a partial charge transfer from underlying Cu to empty π^* states of the upper Dirac cone. The filling of these states can be observed in the dispersion relations displayed in figures 7 and 8(a). The spectra and dispersions shown in figures 3, 7 and 8(a) identify the corresponding shifts of the Dirac point as well as of the bottom and the top of the π band toward higher binding energies by 0.3 and 0.4 eV, respectively, as compared to the case of intercalated Au (figures 2 and 4(a)). In [35, 36] the shift of the Dirac point upon contacting graphene to different metals

(Pt, Au, Cu, Ag and Al) has been analyzed in the framework of local density calculations. These works have revealed a correlation between the resulting energy positions of the Dirac point and the differences in work functions of metallic substrates and graphene. Later, such a correlation was confirmed by photoemission experiments with graphene intercalated with Au, Ag and Cu [27]. The energetic positions of Dirac points in the Au- and Cu-intercalated graphene seen in figures 4(a) and 8(a) correlate well with the calculations presented in [35, 36] and confirm the conclusion about partial charge transfer between graphene and intercalated Cu. At the same time, we have to remark that in the studies [35, 36] an opening of a band gap between π and π^* states of graphene was not detected.

In accordance with the analysis presented in [37], the appearance of the energy gap between Dirac cones in graphene can be related to the distortion of the graphene structure and the breaking of the graphene sublattice symmetry (A–B symmetry) caused by different substrates. One can assume different gap values to result from different structural parameters of graphene and its substrate. Analysis of the band gap width for the case of graphene intercalated with Au, Ag and Cu shows that the gap is largest for Ag, medium for Cu and minimal (close to zero) for Au [27]. At the same time, the systems with intercalated monolayers of Au and Ag are characterized by almost incommensurate p (9×9) and p (7×7) structures, respectively, thus revealing remarkable differences between lattice constants of graphene and the intercalated metallic layers [38–40]. In the case of the Cu intercalation, the formation of a structure close to p (1×1) takes place [27, 41]). Different values of the band gap in Au-, Ag- and Cu-intercalated graphene can be ascribed to the influence of two factors: (i) charge transfer and (ii) distortion of graphene due to misfit of its crystal structure with the structure of the intercalated material. Since the interaction between graphene and intercalated Cu and Ag is stronger due to partially ionic bonding between graphene and metallic layers, the mismatch between crystalline parameters plays a significant role for these substrates. The mismatch becomes increasingly important with increasing transferred charge. The gap in Ag-intercalated graphene is larger and this correlates with the larger energy shift of the π band and a higher amount of charge transfer. In the case of intercalated Au the charge transfer is negligible, the bonding is weaker and the influence of the structural mismatch between graphene and Au is not strong. As a result the gap in Au-intercalated graphene tends to zero.

As seen from figure 5, in the crossing region of the graphene and Au d states, the spin splitting strongly increases [11]. It is important to understand what can be the origin of such a significant modification of the spin structure. A possible explanation of this point can be offered in the context of spin-dependent avoided crossing. The essence of this effect is as follows. Since the spin subbands of the electronic states in the substrate (i.e. intercalated Au layer) are originally split, each graphene state with a given spin will couple to the d states of the substrate with the same spin. The bands of emerging hybridized (π–d) states with a given spin orientation will energetically follow the Au d states with the corresponding spin. It is evident from figure 5 that outside the energy–momentum frame where π and Au d states are crossing (i.e. polar angles of 7–10° and 23–25°, $k_{\|}$ intervals of 0.3–0.6 and 1.5–1.7 Å^{-1}, respectively) Au 5d states at binding energies of ∼3.5–4.5 eV exhibit a clearly pronounced spin splitting. The energy separation between these states is ∼0.7 eV, which practically reaches the value of the intrinsic spin–orbit splitting of d states of Au (see figure 6(a)).

To verify the assumption that the Au 5d states are originally spin split and the splitting is not related to the presence of graphene on top, we have studied a monolayer of Au on Ni(111) without graphene. Graphene was removed from the sample by annealing at 800–850 K.

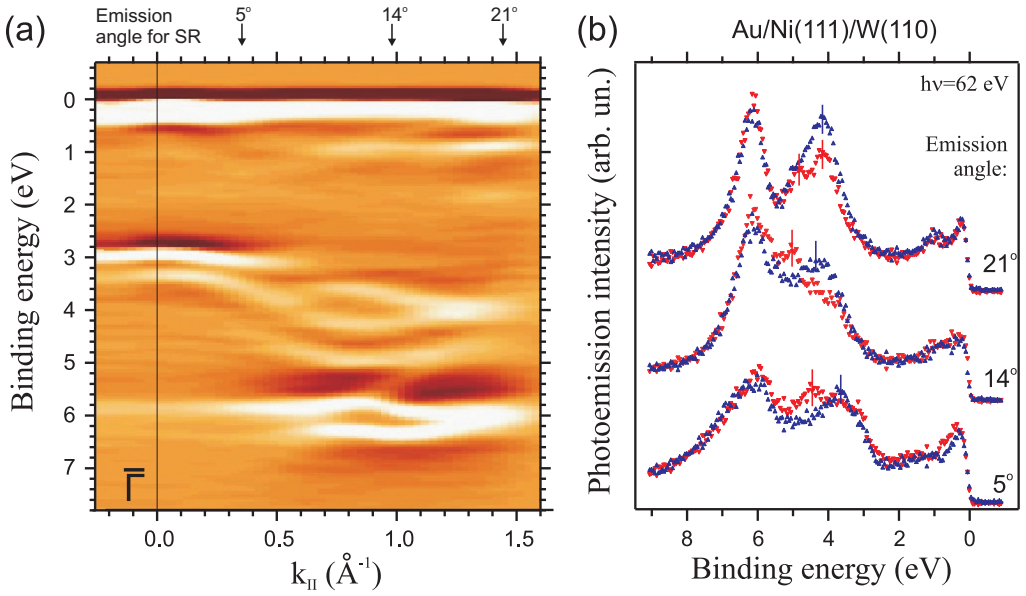

Figure 11. (a) Dispersion of Au d states in a system with Au overlayer on the Ni(111) surface and (b) the corresponding spin-resolved photoemission spectra measured at different polar angles to the surface normal. The contributions due to different spin directions are identified with red and blue colours. Arrows indicate the polar angles for which spin-resolved spectra have been measured.

Figure 11(a) displays spin-integrated dispersions of electronic states for the bare monolayer of Au on Ni(111) and figure 11(b) shows selected spin-resolved photoemission spectra obtained for this system.

We clearly see that the spin structure of Au d states in the monolayer of Au on Ni(111) without graphene is similar to that observed for Au/Ni(111) with graphene on top. On the other hand, dispersions of d bands differ from those characteristic of the (111) face of the single crystal of Au [42]. This is quite explainable since the monolayer of Au on top of Ni(111) forms a p (9×9) structure due to ∼16% lattice mismatch between Au and Ni (lattice constant of 4.079 Å for Au versus 3.524 Å for Ni) [38–40]. Spin-resolved spectra for this system (figure 11(b)) reveal a pronounced spin polarization of the Au d states at binding energies of ∼3.5–4.5 eV. The energies of these spin-split states are close to those observed in the system with the graphene overlayer. Thus we conclude that the interaction between the π band of graphene and these spin-polarized states account for the significant spin splitting of the hybridized d–π states (figures 5 and 6(a)).

For theoretical calculations of the spin structure and magnitude of the spin–orbit splitting of the π states of graphene on Au, please see our earlier publication [11]. It was shown there that a key factor for the creation of a large spin–orbit splitting in graphene is hybridization of the p_z states of graphene with the $5d_{z^2}$ states of Au and that spin splitting increases with the degree of hybridization between these states. Theory [11] suggests that outside the energy–momentum region where the graphene band is crossing with Au d states, the spin–orbit splitting can be as high as ∼100 meV, which is confirmed by our experiments. The theoretical calculations from [43, 44] also support the possibility of achieving an anomalously large spin–orbit splitting in graphene upon contact with Au.

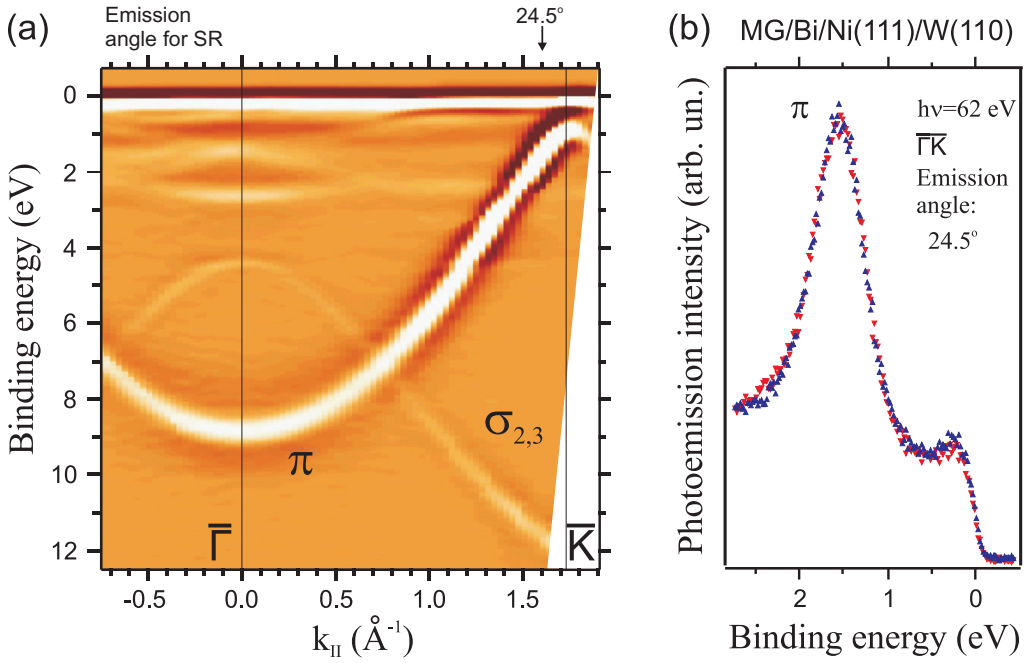

Figure 12. Dispersion of valence band electronic states of graphene along the $\bar{\Gamma}\bar{K}$ direction of the Brillouin zone measured for a graphene monolayer intercalated by Bi, and (b) the corresponding spin-resolved photoemission spectrum measured for the values of $k_{\|}$ in the region of the linearity of the dispersion of the π states of graphene. The contributions due to different spin directions are identified with red and blue colors. The arrow indicates the polar angle for which the spin-resolved spectrum has been measured.

To confirm the importance of the d–π hybridization for the induced spin–orbit splitting of π states of graphene, we have performed comparative experiments with intercalation of Bi under graphene on Ni(111). Bi is a metal with a high atomic number, but with an sp-type valence band without d electrons. In figure 3, the normal emission spectrum of Bi-intercalated graphene is shown. The binding energy of π states is similar to the cases of graphene on Au and Cu. At the same time, Bi-derived features occur at binding energies of about 2.5 and 1.5 eV, and the background of Ni d states is seen at the Fermi level. Deposition of a large amount of Bi (3–4 monolayers) on top of graphene prior to annealing at 300 °C was necessary for the formation of a complete layer of Bi between graphene and Ni(111).

A complete interlayer of Bi was not achievable when concentrations lower than 3 ML were deposited. Such samples show two peaks of π states at binding energies of about 10 and 8.8 eV. For the samples in which only one π state was observed at 8.8 eV, additional intercalation of noble metals was not possible, which confirms that the space between graphene and Ni(111) substrate is fully occupied by Bi atoms. Only after partial de-intercalation of Bi was additional intercalation of noble metals possible. Figure 12(a) shows the corresponding dispersion of the π states of Bi-intercalated graphene which were measured along the $\bar{\Gamma}\bar{K}$ direction of the SBZ. One can clearly see the overall energy shift of the π band toward lower binding energy (as compared to bare graphene on Ni in figure 1), which demonstrates a blocking of the strong interaction between graphene and Ni(111) by the Bi interlayer.

A minor shift of the Dirac point toward higher binding energy (as compared to the case of Au-intercalated graphene) along with the opening of a small band gap are also observed. These experimental observations can be explained in the same manner as for noble metals, i.e. by the mismatch between crystal structures of graphene and intercalated Bi. The Bi-derived features can be distinguished in figure 12(a) by their characteristic dispersions in the energy region between 1.5 and 2.5 eV at the $\bar{\Gamma}$ point. Such dispersions are not observed for the bare graphene/Ni(111) system.

It is important to note that the photoemission data shown in figure 12(a) reveal no hybridization-like modification of the π band, like that observed for Au- and Cu-intercalated graphene in the energy region of d states. Figure 12(b) shows a spin-resolved photoemission spectrum of the π band, acquired in the vicinity of the Fermi energy close to the $\bar{K}$ point of the SBZ. It is clearly seen that the π band is not spin split. This means that despite the high atomic number of the intercalated material the contact of graphene with Bi does not induce any measurable spin polarization in the π states. Hence, the hybridization of π states of graphene with d states of the contact metal is a crucial factor.

5. Conclusion

Let us now summarize the results of the present study:

1. Intercalation of Au atoms under graphene synthesized on the Ni(111) surface recovers the electronic structure characteristic of free-standing graphene, with linear dispersion of π states in the vicinity of the $\bar{K}$ point of the SBZ and the Dirac point close to the Fermi energy.
2. Interaction of graphene with the intercalated Au leads to hybridization between π states of graphene and 5d states of Au. Since the Au 5d states are located at the binding energies above 2.5 eV, both hybridized (d–π) bonding and (d–π)* antibonding states emerge below the Fermi level and exhibit comparable population. This accounts for the overall weak coupling between graphene and intercalated Au layer. This is also in clear contrast to the case of graphene on the Ni(111) surface, where hybridized (d–π)* antibonding states occur above the Fermi level, which accounts for the strong coupling between graphene and the Ni substrate.
3. The hybridization of graphene π states with the 5d states of Au is responsible for the creation of a large spin–orbit splitting in the π band of graphene. In the energy region where the π band of graphene crosses the 5d states of Au, the graphene states couple to the Au states with the same spin orientation, which results in a spin splitting of the π states of up to 0.6–0.7 eV. Outside the band crossing area, in the region where the π band dispersion is linear, the spin splitting of the π states is constant with a magnitude of $\sim$100 meV. The Au d states that interact with the π states of graphene are spin–orbit split by themselves. The resulting modification of the spin structure of π states can be explained in terms of a spin-dependent avoided crossing effect between d and sp states of Au and π states of graphene.
4. In the case of Cu-intercalated graphene, the electronic structure of the system is slightly different. In addition to an overall energy shift of the valence band toward lower binding energy, as compared to the bare graphene on Ni(111), intercalation of Cu results in the formation of a small energy gap between the π and π^* states, accompanied by the

occurrence of a spectral feature at the Fermi level due to partial filling of the graphene π^* states. In the region of crossing of graphene π states with the 3d states of Cu, one also observes distortions of the π state dispersion, which can be assigned to the hybridization between the π band of graphene and Cu 3d state. This interaction does not, however, culminate in any induced spin–orbit splitting of the π states. This can be explained as due to the small atomic number of Cu and, accordingly, the low intrinsic spin–orbit interaction of the Cu d states.

5. Intercalation of the heavy metal Bi under graphene in Ni(111) also leads to an overall energy shift of the π states toward the Fermi level accompanied by the formation of a small energy gap at the Dirac point. However, this does not cause any noticeable induced spin splitting in the π band due to the absence of d states in the valence band of Bi, which could effectively hybridize with the π states of graphene.

Acknowledgments

This work was supported by a grant from St Petersburg University for scientific investigations 'Synthesis and electronic and spin structure of graphene on different substrates' and the RFBR project (11-02-00642-a), and was performed in the framework of a collaboration between the Deutsche Forschungsgemeinschaft and the Russian Fund for Basic Research (11-02-91344 and RA 1041/3-1). The authors acknowledge support from the Russian–German laboratory at BESSY and the program 'German–Russian Interdisciplinary Science Center' (G-RISC).

References

[1] Novoselov K S, Geim A K, Morozov S V, Jiang D, Zhang Y, Dubonos S V, Grigorieva I V and Firsov A 2004 *Science* **306** 666
[2] Geim A K 2009 *Science* **324** 1530
[3] Geim A K and Novoselov K S 2007 *Nature Mater.* **6** 183
[4] Novoselov K S, Geim A K, Morozov S V, Jiang D, Katsnelson M I, Grigorieva I V, Dubonos S V and Firsov A A 2005 *Nature* **438** 197
[5] Katsnelson M I, Novoselov K S and Geim A K 2006 *Nature Phys.* **2** 620
[6] Castro Neto A H, Guinea F, Peres N M R, Novoselov K S and Geim A K 2009 *Rev. Mod. Phys.* **81** 109
[7] Ohta T, Bostwick A, Seyller T, Horn K and Rothenberg E 2006 *Science* **313** 951
[8] Bostwick A, Ohta T, Seyller T, Horn K and Rothenberg E 2007 *Nature Phys.* **3** 36
[9] Geim A K and MacDonald A H 2007 *Phys. Today* **60** 35
[10] Varykhalov A, Sánchez-Barriga J, Shikin A M, Biswas C, Vescovo E, Rybkin A, Marchenko D and Rader O 2008 *Phys. Rev. Lett.* **101** 157601
[11] Marchenko D, Varykhalov A, Scholz M R, Bilmayer G, Rashba E I, Rybkin A, Shikin A M and Rader O 2012 *Nature Commun.* **3** 1232
[12] Kane C L and Mele E J 2005 *Phys. Rev. Lett.* **95** 226801
[13] Shikin A M, Varykhalov A, Prudnikova G V, Usachov D, Yamada Y, Riley J D and Rader O 2008 *Phys. Rev. Lett.* **100** 057601
[14] Varykhalov A, Sánchez-Barriga J, Shikin A M, Gudat W, Eberhardt W and Rader O 2008 *Phys. Rev. Lett.* **101** 256601
[15] Shikin A M, Rybkin A G, Marchenko D E, Usachov D Yu, Adamchuk V K, Varykhalov A Yu and Rader O 2010 *Phys. Solid State* **52** 1515

[16] Rybkin A G, Shikin A M, Adamchuk V K, Marchenko D, Bismas C, Varykhalov A and Rader O 2010 *Phys. Rev.* B **82** 233403
[17] Rybkin A G, Shikin A M, Marchenko D, Varykhalov A and Rader O 2012 *Phys. Rev.* B **85** 045425
[18] Shikin A M, Farias D and Rieder K H 1998 *Europhys. Lett.* **44** 44
[19] Shikin A M, Farias D, Adamchuk V K and Rieder K H 1999 *Surf. Sci.* **424** 155
[20] Farias D, Shikin A M, Rieder K H, Adamchuk V K, Tanaka T and Oshima C 2000 *Surf. Sci.* **454–456** 437
[21] Farias D, Shikin A M, Rieder K H and Dedkov Yu S 1999 *J. Phys.: Condens. Matter* **11** 8453
[22] Shikin A M, Prudnikova G V, Adamchuk V K, Moresco F and Rieder K H 2000 *Phys. Rev.* B **62** 13202
[23] Dedkov Yu S, Shikin A M, Adamchuk V K, Molodtsov S L, Laubshat C, Bauer A and Kaindl G 2001 *Phys. Rev.* B **64** 035405
[24] Starodubov A G, Medvetski M A, Shikin A M and Adamchuk V K 2004 *Phys. Solid State* **46** 1340
[25] Shikin A M, Adamchuk V K and Rieder K-H 2009 *Phys. Solid State* **51** 2390
[26] Sánchez-Barriga J, Varykhalov A, Scholz M R, Rader O, Marchenko D, Rybkin A, Shikin A M and Veskovo E 2010 *Diamond Relat. Mater.* **19** 734
[27] Varykhalov A, Scholz M R, Kim T K and Rader O 2010 *Phys. Rev.* B **82** 121101
[28] Rader O, Varykhalov A, Sánchez-Barriga J, Marchenko D, Rybkin A and Shikin A M 2009 *Phys. Rev. Lett.* **102** 057602
[29] Marchenko D, Varykhalov A, Rybkin A, Shikin A M and Rader O 2011 *Appl. Phys. Lett.* **98** 122111
[30] Gierz I *et al* 2010 *Phys. Rev.* B **81** 235408
[31] Enderlein C, Kim Y S, Bostwick A, Rotenberg E and Horn K 2010 *New J. Phys.* **12** 033014
[32] Bertoni G, Calmels L, Altibelli A and Serin V 2005 *Phys. Rev.* B **71** 075402
[33] Dedkov Yu S and Fonin M 2010 *New J. Phys.* **12** 125004
[34] Walter A L, Nie S, Bostwick A, Kim K S, Moreschini L, Chang Y J, Innocenti D, Horn K, McCarty K F and Rotenberg E 2011 arXiv:1108.2066v1 [cond-mat.mes-hall]
[35] Giovannetti G, Khomyakov P A, Brocks G, Karpan V M, Brink J and Kelly P J 2008 *Phys. Rev. Lett.* **101** 026803
[36] Khomyakov P A, Giovannetti G, Rusu P C, Brocks G, Brink J and Kelly P J 2009 *Phys. Rev.* B **79** 195425
[37] Abdelouahed S, Ernst A, Henk J, Maznichenko I V and Mertig I 2010 *Phys. Rev.* B **82** 125424
[38] Jones T E, Noakes T C Q, Bailey P and Baddeley C J 2006 *Surf. Sci.* **600** 2129
[39] Jacobsen J, Pleth Nielsen L, Besenbacher F, Stensgaard I, Lagsgaard E, Rasmussen T, Jacobsen K W and Norskov J K 1995 *Phys. Rev. Lett.* **75** 489
[40] Umezawa K, Nakanishi S and Gibson W 1998 *Phys. Rev.* B **57** 8842
[41] Koschek H, Held G, Trischberger P, Widdra W, Birkenheuer U and Steinruek H-P 1999 *Appl. Surf. Sci.* **142** 18
[42] Hüfner S 1995 *Photoelectron Spectroscopy: Principles and Applications* (Berlin: Springer)
[43] Li Z Y, Yang Z Q, Qiao S, Hu J and Wu R Q 2011 *J. Phys.: Condens. Matter* **23** 225502
[44] Ma D, Li Z and Yang Z 2012 *Carbon* **50** 297